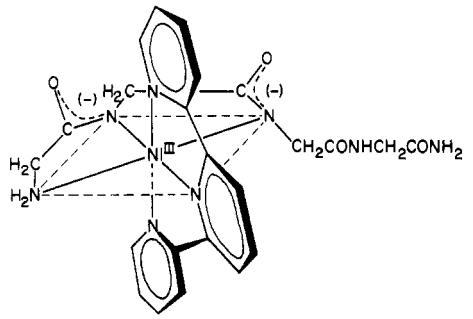

VIII, $[Ni^{III}(H_{-2}G_4a)(terpy)]^+$

splitting of g_{zz} into five peaks (A_{zz} = 20.0 G) shows two equivalent axial nitrogens are present. The equatorial plane is defined by the strongest donors, which are the amine nitrogen, two deprotonated peptide nitrogens, and one pyridyl nitrogen from terpy. The elongated axis has the two terminal pyridyl nitrogens from terpy. The g_{av} value decreases significantly to a value of only 2.113 for these terpy adducts.

Conclusions

Systematic changes in isotropic and anisotropic EPR spectra (and the corresponding **g** tensors) permit structural assignments to be made for nickel(III) peptide complexes as a function of acidity and in the presence of other chelating ligands. The substitution lability of the six coordination positions of nickel(III) differ greatly. Previous work[3,21] has shown that the elongated axial donors are extremely labile. This work shows that one of the equatorial positions is relatively labile. Carboxylate or peptide nitrogen groups coordinated in the fourth equatorial position (from the terminal amine of the peptide) undergo substitution and protonation reactions much more rapidly (by factors of 10^3 or more) than the other coordinated groups (an amine and two deprotonated peptide nitrogens). The changes in EPR spectra and the kinetics of the reactions in acid provide evidence for peptide oxygen protonation of the nickel(III) peptide complexes.

Acknowledgment. This work was supported by Public Health Service Grant No. GM-12152 from the National Institutes of General Medical Sciences. The assistance of Dr. George E. Kirvan in the preparation of the manuscript is appreciated.

Contribution from the Department of Chemistry, Purdue University, West Lafayette, Indiana 47907

Polypyridine and Polyamine Mixed-Ligand Complexes of Tripeptidonickel(III)

THOMAS L. PAPPENHAGEN, WILLIAM R. KENNEDY, CONRAD P. BOWERS, and DALE W. MARGERUM*

Received August 9, 1985

The GGG, GAG, and GGA tripeptide complexes of nickel(III) undergo substitution reactions with en, dien, bpy, phen, and terpy to form relatively stable chelated ternary complexes. Peptide complexes with Aib (α-aminoisobutyric acid) in the third residue are sterically hindered in the formation of chelate adducts. Thus, $Ni^{III}(H_{-2}Aib_3)(H_2O)_2$ does not form polypyridine adducts and forms only monodentate axially coordinated polyamine adducts. EPR spectra of frozen aqueous solutions show that the $Ni^{III}(H_{-2}GGA)$dien complex can exist in three forms. Dien is monodentate with axial Ni(III) coordination below pH 4, it is bidentate at pH 7–8 (the GGA carboxylate group is replaced to give five nitrogens coordinated to nickel), and it is tridentate above pH 11 to give the mixed complex with six coordinated nitrogens. $Ni^{III}(H_{-2}GAG)$terpy has six nitrogens coordinated to nickel(III) from pH 2 to pH 11. The stability constant for terpy addition is $10^{12.8}$ M^{-1}. This ternary complex has a reduction potential of 0.56 V (vs. NHE). Terpy also stabilizes the nickel(III) peptide complex in regard to self-redox decomposition reactions in basic solution.

Introduction

Nickel(III) peptide complexes have been characterized by their electrode potentials, EPR and UV–vis spectra, electron-transfer reactions, redox decomposition rates,[1-8] and, more recently EXAFS.[9] The *trans*-diaquanickel(III) tripeptide complexes (e.g. $Ni^{III}(H_{-2}GAG)(H_2O)_2$,[10] structure **1**) and tripeptide amide complexes undergo rapid substitution of axial water molecules to form 1:1 adducts with ammonia, imidazole, or pyridine.[6] These substituted nickel(III) peptide complexes are characterized by an increased kinetic stability to redox decomposition in neutral and basic solution and by a lowered reduction potential when compared

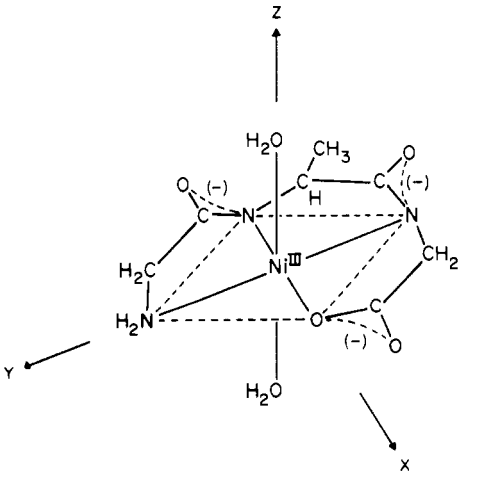

1

with that of the parent nickel(III) peptide complex.

Nickel(III) tris(diimine) complexes (e.g. $Ni(bpy)_3^{3+}$) have been formed in strongly acidic solution[11-13] and in acetonitrile.[14] These

(1) Bossu, F. P.; Margerum, D. W. *J. Am. Chem. Soc.* **1976**, *98*, 4003–4004.
(2) Bossu, F. P.; Margerum, D. W. *Inorg. Chem.* **1977**, *16*, 1210–1214.
(3) Lappin, A. G.; Murray, C. K.; Margerum, D. W. *Inorg. Chem.* **1978**, *17*, 1630–1634.
(4) Sugiura, Y.; Mino, Y. *Inorg. Chem.* **1979**, *18*, 1336–1339.
(5) Sakurai, T.; Hongo, J.; Nakahara, A.; Nakao, Y. *Inorg. Chim. Acta* **1980**, *46*, 205–210.
(6) Murray, C. K.; Margerum, D. W. *Inorg. Chem.* **1982**, *21*, 3501–3506.
(7) Jacobs, S. A.; Margerum, D. W. *Inorg. Chem.* **1984**, *23*, 1195–1201.
(8) Kirvan, G. E.; Margerum, D. W. *Inorg. Chem.* **1985**, *24*, 3245–3253.
(9) Kennedy, W. R.; Powell, D. R.; Niederhoffer, E. C.; Teo, B. K.; Orme-Johnson, W. H.; Margerum, D. W., to be submitted for publication.
(10) GAG is the tripeptide glycyl-L-alanylglycine and H_{-2} refers to the two deprotonated peptide nitrogens coordinated to nickel.
(11) Wells, C. F.; Fox, D. *J. Chem. Soc., Dalton Trans* **1977**, 1498–1501.

0020-1669/85/1324-4356$01.50/0

complexes are not stable at higher pH values and have much more positive reduction potentials than do the peptide complexes.

The present study examines the effect of chelation of bi- and tridentate polyamine and polypyridine ligands upon the stability (thermodynamic and kinetics) of the resulting nickel(III) tripeptide mixed-ligand complexes. Tripeptide complexes of GAG and GGA are used because their nickel(III) complexes are slower to undergo self-redox decomposition than the GGG complexes. The mixed-ligand complexes are similar in structure and properties to the five- and six-nitrogen bis(tripeptido)nickelate(III) complexes.[8] We are interested in ligands that help to stabilize the trivalent oxidation state of nickel and in the nature of the resulting complexes.

Electron paramagnetic resonance (EPR) spectroscopy is very useful in the determination of the structure or coordination sphere of d^7, low-spin nickel(III) peptide complexes.[1,3-9] These complexes are sufficiently unstable that crystal structure determinations have not yet been possible, although EXAFS studies provide some structural information.[9] Nickel(III) peptide complexes, with strong equatorial donors such as deprotonated peptide nitrogens and weaker axial donors such as water or ammonia, prefer a tetragonally elongated geometry. This geometry places the unpaired electron in the d_{z^2} orbital, oriented along the z axis of the molecule. Thus, axial donor atoms with nonzero nuclear spin (e.g. nitrogen-14, $I = 1$) provide additional splitting in the high-field, $g_\parallel$, region of the frozen-solution EPR spectrum. This splitting provides information on the formation of the axial donor complexes.

In the case of (polypyridine)nickel(III) peptide mixed-ligand complexes, interference from the intense nickel(II) polypyridine absorbance hinders UV–vis spectrophotometric characterization of the nickel(III) complexes. Thus, EPR techniques are needed to characterize these complexes. Magnetically dilute frozen aqueous glass EPR has been used extensively as a means of characterizing the nickel(III) coordination sphere as frozen-solution spectra yield more structural information than the aqueous-solution spectra. The frozen-solution spectra, however, tend to distort equilibrium processes, sometimes significantly.[6] Thus, the aqueous-solution spectra were also recorded to verify that the species observed in frozen solution are stable in solution at room temperature.

Experimental Section

Chromatographically pure peptides were obtained from Vega-Fox, Biosynthetika, or Sigma. Di-α-aminoisobutyryl-α-aminoisobutyric acid (Aib_3) was synthesized by A. W. Hamburg, with methods described previously.[15,16] Abbreviations for the amino acid residues: G, glycyl; A, L-alanyl; a, amide.

A stock solution of $Ni(ClO_4)_2$ was prepared from the reaction of $NiCO_3$ and $HClO_4$ and titrated with EDTA to a murexide end point. 2,2′:6′,2″-Terpyridine (terpy) was twice recrystallized from petroleum ether. 2,2′-Bipyridine (bpy) and 1,10-phenanthroline (phen) were used as received. Ethylenediamine (en) and diethylenetriamine (dien) were vacuum-distilled.

Solutions of nickel(II) peptides (2×10^{-3} M) were prepared by the reaction of 10–20% excess peptide with $Ni(ClO_4)_2$. Prior to electrolysis the solution was adjusted to pH 9.3–10.0 to ensure full formation of the deprotonated species. The ionic strength was maintained at 0.1 with either $NaClO_4$ or $NaNO_3$. Nickel(II) peptide solutions were used within 48 h of their preparation and refrigerated to help prevent base hydrolysis of the peptide. In the case where the peptide was Aib_3, the pH was lowered to ~7 immediately prior to electrolysis.

Nickel(III) peptide solutions were prepared by electrochemical oxidation of the corresponding nickel(II) complex with use of a flow-through bulk electrolysis column.[17,18] The nickel(III) peptide solutions were stored in the dark under slightly acidic conditions (pH ~3) in order to minimize redox decomposition. Mixed-ligand complexes were prepared by the reaction of nickel(III) peptide solutions (typically $(1-2) \times 10^{-3}$ M) with solutions of ligand (10^{-3}–0.05 M), after which the pH and ionic strength were adjusted to the desired conditions.

Table I. Broadening Parameters from the EPR Simulations of Nickel(III) Complexes in Frozen Aqueous Solution at −150 °C

complex	W_{xx}	W_{yy}	W_{zz}
$Ni^{III}(H_{-2}GGA)(H_2O)_2$	21.0	16.0	6.5
$Ni^{III}(H_{-2}GGA)(H_2O)en$[a]	21.0	17.0	6.7
$Ni^{III}(H_{-2}GGA)(en)_2$[a,b]	12.0	11.0	6.2
$Ni^{III}(H_{-2}GGA)(H_2O)dien$[a]	20.0	15.0	5.8
$Ni^{III}(H_{-2}GGA)(H_2O)dien$[b]	12.5	11.0	5.8
$Ni^{III}(H_{-2}GGA)dien$[c]	13.0	17.9	7.1
$Ni^{III}(H_{-2}Aib_3)(H_2O)_2$	22.0	17.0	7.5
$Ni^{III}(H_{-2}Aib_3)(H_2O)en$[a]	17.6	13.5	5.3
$Ni^{III}(H_{-2}Aib_3)(H_2O)dien$[a]	19.5	12.7	5.7
$Ni^{III}(H_{-2}GAG)(H_2O)_2$	24.0	18.5	7.5
$Ni^{III}(H_{-2}GAG)(H_2O)bpy$[b]	14.1	14.1	5.3
$Ni^{III}(H_{-2}GAG)(H_2O)phen$[b]	14.0	14.0	5.1
$Ni^{III}(H_{-2}GAG)(H_2O)Ph_2phen$[b]	14.0	14.0	5.0
$Ni^{III}(H_{-2}GAG)terpy$[c]	11.0	11.0	5.2

[a] Monodentate. [b] Bidentate. [c] Tridentate.

Electron paramagnetic resonance spectra were obtained with a Varian E-109 X-band EPR spectrometer modulated at 100 kHz. For frozen-solution work, spectra of magnetically dilute aqueous glasses (nickel(III) peptide concentrations less than 1×10^{-3} M) were recorded with a Varian E-231 variable-temperature cavity and a Varian E-238 variable-temperature controller. Unless otherwise stated, these spectra were recorded at −150 ± 3 °C and at 9.08 GHz. The magnetic field was calibrated relative to α,α'-diphenyl-β-picrylhydrazyl (DPPH), $g_{iso} = 2.0037$.

Hyperfine coupling constants (A), broadening parameters (W), and g values were determined from a computer-generated spectral matching procedure.[3,19] Broadening parameters are given in Table I. Frozen EPR spectra of *trans*-diaquatetracyanonickelate(III) mixed-ligand complexes[20] show that appreciable splitting from axial nitrogen donors can be observed in the $g_\perp$ region as well as the $g_\parallel$ region for these tetragonally elongated nickel(III) species. Although $g_\perp$ splitting is not observed for the nickel(III) peptide mixed-ligand complexes, hyperfine coupling constants along the equatorial axes, A_{xx} and A_{yy}, are needed to fit the line shape. Spectral simulations begin with the assumption that A_{xx} and A_{yy} are 80% of the more easily discernible A_{zz} value. Then these A values are varied along with the broadening parameters until the best fit is obtained. This improved the match of the simulated spectra with the experimental spectra. The g values and A values for the mixed-ligand complexes are given in Table II. The precision of the g values is ±0.002 for g_{zz}, ±0.003 for $g_{xx} \neq g_{yy}$, and ±0.004 for $g_{xx} = g_{yy} = g_\perp$.

Room-temperature EPR spectra were obtained at 9.40 GHz with a Varian E-238 multipurpose cavity and a thin (0.1-mm) quartz cell (Wilmad). Room-temperature aqueous titrations were performed with EPR detection. A peristaltic pump (Gilson) was used to circulate the solution through a thin quartz cell in the EPR multipurpose cavity and back to the titration beaker. If the EPR cell is not moved and the ionic strength of the solution remains constant, the height of the derivative signal is proportional to the concentration of the paramagnetic species. This was verified by dilution of a stable copper(II) solution. A plot of the copper(II) concentration vs. the concentration calculated from the height of the derivative signal gave a slope of 1.01 ± 0.01 ($r^2 > 0.999$) over the concentration range of interest.

Ultraviolet–visible spectra were recorded on either a Cary 14, a Hewlett Packard HP8450A, or a Perkin-Elmer 320 spectrophotometer. The latter was equipped with a Perkin-Elmer 3600 Data Station. Reaction rates were measured under pseudo-first-order conditions with a Cary 16 or Durrum stopped-flow spectrophotometer[21] at 25.0 ± 0.1 °C. The decomposition of $Ni^{III}(H_{-2}GAG)terpy$ was measured at 360 nm, a region of the spectrum free of interference from $Ni(terpy)_2^{2+}$. The UV–vis spectrum of $Ni^{III}(H_{-2}GAG)terpy$ was obtained with a circulating system consisting of a small column with 8 cm^3 of Bio-Rad AG-50 cation-exchange resin, a peristaltic pump, and a flow-through UV–vis

(12) Wells, C. F.; Fox, D. *J. Chem. Soc., Dalton Trans* **1977**, 1502–1504.
(13) Brown, J. K.; Fox, D.; Heyward, M. P.; Wells, C. F. *J. Chem. Soc., Dalton Trans* **1979**, 735–739.
(14) Brodovitch, J. C.; Haines, R. I.; McAuley, A. *Can. J. Chem.* **1981**, *59*, 1610–1614.
(15) Hamburg, A. W.; Nemeth, M. T.; Margerum, D. W. *Inorg. Chem.* **1983**, *22*, 3535–3541.
(16) Kirksey, S. T.; Neubecker, T. A.; Margerum, D. W. *J. Am. Chem. Soc.* **1979**, *101*, 1631–1633.
(17) Murray, C. K.; Margerum, D. W. *Inorg. Chem.* **1983**, *22*, 463–469.
(18) Clark, B. R.; Evans, D. H. *J. Electroanal. Chem.* **1965**, *69*, 181–194.
(19) Toy, A. D.; Chaston, S. H. H.; Philbrow, J. R.; Smith, T. D. *Inorg. Chem.* **1971**, *10*, 2219–2226.
(20) Pappenhagen, T. L.; Margerum, D. W. *J. Am. Chem. Soc.* **1985**, *107*, 4576–4577.
(21) Willis, B. G.; Bittikofer, J. A.; Pardue, H. L.; Margerum, D. W. *Anal. Chem.* **1970**, *42*, 1340–1349.

Table II. Hyperfine Coupling Constants (A Values) and g Values for Nickel(III) Tripeptide Polyamine and Polypyridine Mixed-Ligand Complexes in Frozen Aqueous Solution at −150 °C

	g_{xx}	$g_{\perp}$[a]	g_{yy}	g_{zz}	g_{av}	A_{xx}	A_{yy}	A_{zz}
$Ni^{III}(H_{-2}GGA)(H_2O)_2$	2.238		2.289	2.008	2.178			
$Ni^{III}(H_{-2}GGA)(H_2O)en$[b]	2.212		2.255	2.012	2.160	18.0	18.0	23.8[e]
$Ni^{III}(H_{-2}GGA)(en)_2$[b,c]		2.148		2.023	2.106	14.0	14.0	18.5[f]
$Ni^{III}(H_{-2}GGA)(H_2O)dien$[b]	2.210		2.254	2.010	2.158	17.0	17.0	23.6[e]
$Ni^{III}(H_{-2}GGA)(H_2O)dien$[c]	2.145		2.176	2.019	2.113	17.0	17.0	20.1[e]
$Ni^{III}(H_{-2}GGA)dien$[d]		2.161		2.019	2.114	17.8	17.8	20.0[f]
$Ni^{III}(H_{-2}Aib_3)(H_2O)_2$	2.253		2.306	2.010	2.190			
$Ni^{III}(H_{-2}Aib_3)(H_2O)NH_3$	2.215		2.269	2.011	2.165	17.0	17.0	23.8[e]
$Ni^{III}(H_{-2}Aib_3)(NH_3)_2$	2.164		2.212	2.020	2.132	14.0	14.0	18.4[f]
$Ni^{III}(H_{-2}Aib_3)(H_2O)en$[b]	2.226		2.277	2.010	2.171	19.3	19.3	24.5[e]
$Ni^{III}(H_{-2}Aib_3)(H_2O)dien$[b]	2.218		2.268	2.011	2.166	18.0	18.0	24.1[e]
$Ni^{III}(H_{-2}GAG)(H_2O)_2$	2.237		2.291	2.010	2.179			
$Ni^{III}(H_{-2}GAG)(H_2O)bpy$[c]		2.190		2.017	2.132	18.6	18.6	23.2[e]
$Ni^{III}(H_{-2}GAG)(H_2O)phen$[c]		2.190		2.016	2.132	18.4	18.4	23.1[e]
$Ni^{III}(H_{-2}GAG)(H_2O)Ph_2phen$[c]		2.190		2.015	2.132	19.0	19.0	23.0[e]
$Ni^{III}(H_{-2}GAG)terpy$[d]		2.168		2.018	2.117	16.7	16.7	19.8[f]
$Ni^{III}(H_{-3}G_3a)(H_2O)_2$[g]	2.310		2.281	2.006	2.199			
$Ni^{III}(H_{-3}G_3a)(H_2O)(NH_3)$[g]		2.217		2.011	2.148	*i*	*i*	23.4[e]
$Ni^{III}(H_{-3}G_3a)(NH_3)_2$[g]		2.178		2.019	2.125	*i*	*i*	19.0[f]
$Ni^{III}(H_{-2}GAG)(H_{-1}GAG)(H_2O)^{2-}$[c,h]			2.194	2.020	2.136	15.4	15.4	20.7[e]
$Ni^{III}(H_{-2}GAG)_2^{3-}$[d,h]		2.152		2.022	2.109	17.0	17.0	19.8[f]

[a] g_{xx} and g_{yy} values cannot be distinguished. [b] Monodentate. [c] Bidentate. [d] Tridentate. [e] $g_{\parallel}$ triplet. [f] $g_{\parallel}$ quintet. [g] Reference 3. [h] Reference 6. [i] Not calculated.

cell. The HP8450A spectrophotometer was used for rapid (≥1 s) scans. The resin removed any $Ni(terpy)_2^{2+}$ in the solution and permitted the uncharged nickel(III) species to circulate into the cell.

Electrochemical measurements were performed with a three-electrode system with a NaCl saturated calomel reference electrode, a platinum-wire auxiliary electrode, and either a glassy-carbon or carbon-paste working electrode. A Bioanalytical Systems, Inc., BAS 100 instrument was used to generate voltammograms.

The pH was measured with an Orion pH meter and a Corning combination pH electrode. The electrode was calibrated to give the following relationship (μ = 0.1):

$$-\log [H^+] = 0.97pH + 0.26$$

Results and Discussion

Steric Effects of Tripeptide on the Formation of Ternary Complexes. The triglycine, GGA, and GAG complexes of nickel(III) react with bpy, phen, terpy, en, and dien to form ternary complexes where the added ligands are chelated as will be seen from EPR evidence. On the other hand, the $Ni^{III}(H_{-2}Aib_3)(H_2O)_2$ complex does not form bpy, phen, or terpy complexes and forms axially coordinated monodentate complexes with en and dien, which are observed only in frozen solution. Thus, the presence of two α-carbon methyl groups in the third peptide residue blocks chelation of these ligands. Models show that when the terminal carboxylate group is rotated away from its equatorial coordination site, one or both of the methyl groups of the third Aib residue are rotated into positions close enough to this site to sterically hinder the coordination of other ligands. (By contrast, the axial coordination site of the Aib_3 complex is relatively unhindered, despite the presence of three pairs of methyl groups in the peptide backbone.) Steric hindrance by Aib peptides also was observed in the case of nickel(III) bis(tripeptide) complexes.[8] The frozen-solution EPR spectra of the complexes are used to show evidence of ternary complex formation and to assign structures.

Nickel(III) peptide complexes are low-spin d^7 species, and EPR studies show these molecules prefer a tetragonally elongated geometry ($g_{xx} \sim g_{yy} > g_{zz}$) with the unpaired electron in the metal d_{z^2} orbital. Axial donor groups with nonzero nuclear spin quantum numbers cause additional splitting in the high-field g_{zz} ($g_{\parallel}$) and the low-field $g_{\perp}$ region.

Table II gives the g values and the hyperfine coupling constants for several nickel(III) peptide complexes. Ammonia forms 1:1 and 2:1 axial adducts with $Ni^{III}(H_{-3}G_3a)(H_2O)_2$ in the frozen state.[3] This work shows that similar ammine adducts are formed with the $Ni^{III}(H_{-2}Aib_3)(H_2O)_2$ complexes. These complexes are tetragonal, and we assign the EPR axes to be coincident with the coordination axes, where x and y are in the equatorial plane of the metal and peptide donor atoms and the z axis is perpendicular to this plane (structure **1**). The y axis is assigned to the amine–nickel–deprotonated peptide nitrogen atoms. The z axis of the diaquanickel(III) peptide complexes contains two water molecules. When one of these waters is replaced by NH_3 to give $Ni^{III}(H_{-2}Aib_3)(H_2O)(NH_3)$, the g_{av} value decreases, and $g_{\parallel}$ (z axis) is split into a 1:1:1 triplet. When two axial NH_3 molecules are present, the g_{av} value decreases further, and $g_{\parallel}$ is split into a 1:2:3:2:1 quintet. The addition of axial amine adducts also shifts g_{xx} and g_{yy} to lower values.

Only 1:1 NH_3 complexes are observed at room temperature. The stability constant varies from 80 to 350 M^{-1} for different peptides.[4] The $Ni^{III}(H_{-2}Aib_3)(H_2O)_2$ complex gives no evidence of en or dien complex formation at room temperature (1.0×10^{-3} M Ni^{III}, 5.0×10^{-2} M L, pH ~5). However, $Ni^{III}(H_{-2}Aib_3)(H_2O)_2$ forms mixed complexes with en and dien in frozen aqueous glasses that have g values similar to those of the 1:1 NH_3 complexes. En and dien appear to have only monodentate coordination to nickel in the Aib_3 complex in contrast to the behavior with the GGA complex. An increase in pH does not result in an increase in the degree of coordination of the ligand. The steric restrictions that arise from the two methyl groups on the third peptide residue of the Aib_3 ligand limit access to the equatorial site where the carboxylate oxygen is coordinated. Hence, en and dien are unable to displace the carboxylate oxygen and form a chelate ring. Without the additional chelate ring, the complex does not have sufficient stability to exist at room temperature. Therefore, no mixed-ligand complexes of the Aib_3 complex are observed at room temperature. In the frozen-solution EPR spectra, the g values for the dien adduct are nearly identical with the g values for NH_3, whereas the en g values indicate weaker axial bonding. This suggests that the latter species may have the adjacent amine group protonated (i.e. Ni^{III}–$NH_2CH_2CH_2NH_3^+$). A single proton added to the dien ligand at pH 5 would be too far removed from the nickel to affect it.

Polyamine Complexes. $Ni^{III}(H_{-2}GGA)(H_2O)_2$ readily forms mixed-ligand complexes with en and dien. These polyamine ligands are able to displace the axially coordinated water molecules as well as the carboxylate oxygen of the tripeptide complex. The coordination of additional donor groups and the formation of additional chelate rings results in enhanced kinetic stability to self-redox reactions in base, relative to that of the parent tripeptide complex. The formation of polyamine mixed-ligand complexes is observed by EPR at room temperature as well as in aqueous

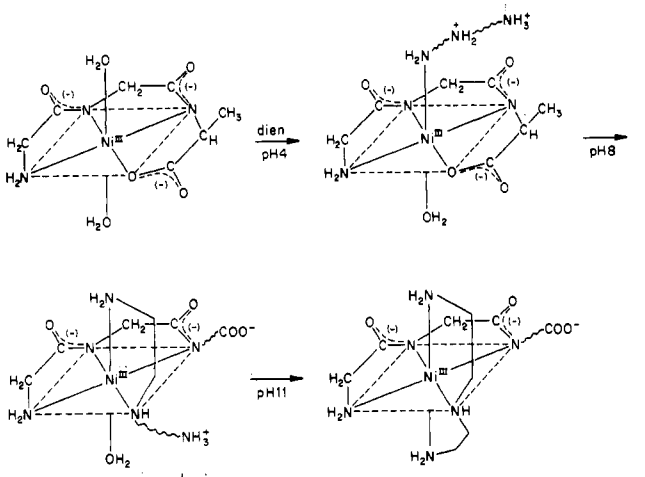

Figure 1. Sequential formation of monodentate, bidentate, and tridentate dien adducts of $Ni^{III}(H_{-2}GGA)$ as the pH is increased. The species are identified from changes in the frozen-solution EPR spectra, and not all species are present in appreciable concentration at room temperature.

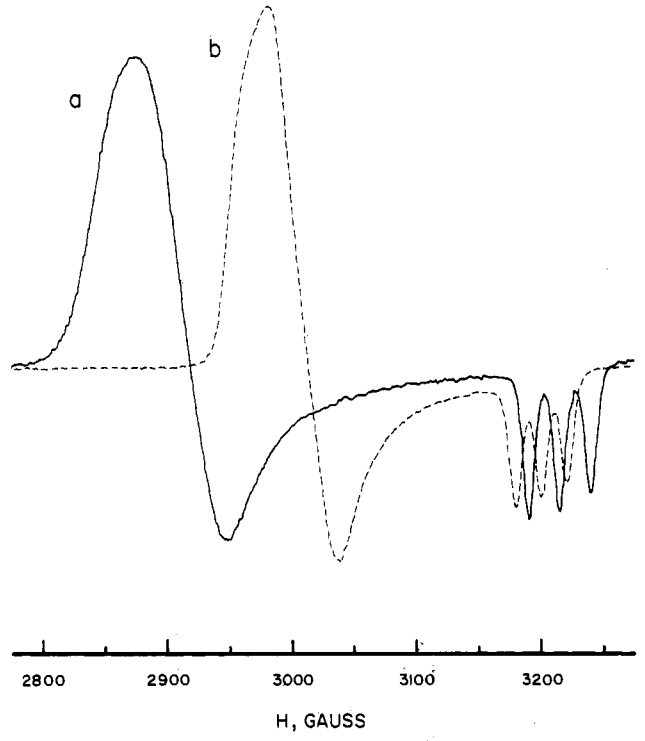

Figure 2. Frozen-aqueous-solution EPR spectra of $Ni^{III}(H_{-2}GGA)(H_2O)$dien complexes at −150 °C and microwave frequency 9.08 GHz (1.0×10^{-3} M $Ni^{III}(H_{-2}GGA)(H_2O)_2$ mixed with 0.1 M dien; μ = 0.1 ($NaClO_4$)): (a) pH 4, monodentate dien; (b) pH 7, bidentate dien.

glasses at −150 °C. The frozen-solution EPR spectra are indicative of tetragonally elongated structures, with $g_{xx} \sim g_{yy} > g_{zz}$.

The EPR spectra of the complexes of $Ni^{III}(H_{-2}GGA)(H_2O)_2$ with dien are consistent with an increased degree of coordination of dien as a function of increased pH (Figure 1). At pH 4, dien has completely displaced one axial water molecule from the tripeptide complex. The resulting monodentate, axially coordinated dien complex is only observed under frozen conditions. As the pH is increased to 7–8, the nitrogen of the central amine of the dien molecule displaces the carboxylate oxygen of the tripeptide. This chelated dien species is found at room temperature and in the frozen glasses. Chelation of the dien brings about a large shift in the equatorial g values (Figure 2 and Table II), as shown by the decrease in g_{av} value from 2.178 for the diaqua complex to 2.158 for the monodentate dien and to 2.113 for the chelated dien complex. This trend is not apparent for the polypyridine ligands, where no monodentate complexes are observed; however, the g_{av} values decrease with an increase in the number of axial N donors. The bidentate dien species is stable at pH 8 for over 24 h. Above pH 11, the EPR of the frozen aqueous solution has a quintet in the g_{zz} region that is consistent with a second, axially coordinated nitrogen that displaces the last water molecule. This indicates a tridentate coordination of dien. This dien complex lasts about 30 s at pH 12 compared to 30 ms in the absence of dien at this pH. This six-nitrogen complex is less stable than the six-nitrogen bis(tripeptido)nickelate(III) or terpy adduct complexes.

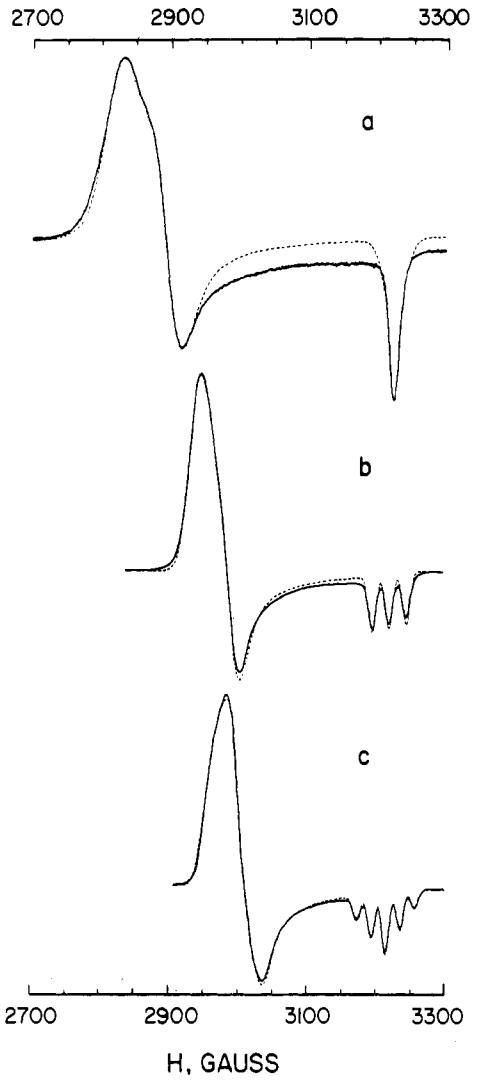

Figure 3. Frozen-aqueous-solution EPR spectra of $Ni^{III}(H_{-2}GAG)(H_2O)_2$ complexes (5×10^{-4} M) at −150 °C, 0.1 M $NaNO_3$, pH 5.0, and microwave frequency 9.08 GHz: (a) $Ni^{III}(H_{-2}GAG)(H_2O)_2$; (b) $Ni^{III}(H_{-2}GAG)(H_2O)$bpy from 5.0×10^{-3} M bpy; (c) $Ni^{III}(H_{-2}GAG)$terpy from 6×10^{-4} M terpy. Solid lines are the experimental spectra; dashed lines are the simulated EPR spectra for the parameters given in Table II.

Mixed-ligand complexes also form with mixtures of $Ni^{III}(H_{-2}GGA)(H_2O)_2$ and en. A monodentate en is fully coordinated in an axial position at pH 6. As the pH is raised to 8, the second nitrogen of the coordinated en displaces the carboxylate oxygen to form a chelate ring and a second en displaces the remaining water in the other axial position. This results in a six-nitrogen species with one monodentate en and one chelated en. This species is stable at room temperature for about 1 h at pH 8.

EPR Spectra of Polypyridine Complexes. The addition of a polypyridine ligand such as terpy or bpy to a sterically unhindered nickel(III) tripeptide solution at pH 3–5 results in the formation of the mixed-ligand complex.[22] Structures are proposed for these

(22) Subak, E. J.; Loyola, V. H.; Margerum, D. W. *Inorg. Chem.*, preceding paper in this issue.

complexes on the basis of their frozen-aqueous-glass EPR spectra. Figure 3 shows the EPR spectra for $Ni^{III}(H_{-2}GAG)(H_2O)_2$ and its bpy and terpy complexes.

Addition of excess bpy to a solution of $Ni^{III}(H_{-2}GAG)(H_2O)_2$ followed by a rapid freeze in liquid nitrogen leads to the EPR spectrum in Figure 3b. The triplet splitting in the g_{zz} or $g_{\parallel}$ region is indicative of one axial nitrogen donor. The g_{av} value decreases from 2.179 to 2.132, and we propose that the bpy is chelated. This complex results from the substitution of one axial H_2O and the displacement of the carboxylate group, the weakest of the four equatorial donors.[22]

The formation of the bpy complex is also observed in aqueous-solution room-temperature EPR spectra with an isotropic room-temperature g value, $g_{iso} = 2.142$, compared with the average g value for the frozen-aqueous-glass EPR simulation, $g_{av} = 2.132$ (Table II). Attempts to add a second bpy with the displacement of the second axial H_2O proved to be unsuccessful. The bpy solubility ($<3.0 \times 10^{-2}$ M) and the steric hindrance of placing a second bpy near the first prevent further coordination.

The EPR spectrum of a frozen solution of terpy and $Ni^{III}(H_{-2}GAG)(H_2O)_2$ is shown in Figure 3c. The quintet of peaks in the $g_{\parallel}$ region indicates the presence of two axial nitrogens. Thus, the proposed structure has a tridentate terpy that coordinates via substitution of the two axial waters and displacement of the equatorial peptide carboxylate group (structure **2**). The aqueous-solution room-temperature EPR of the terpy complex has a g_{iso} value of 2.126, compared with a g_{av} value of 2.117 from the frozen aqueous glass. The aqueous-solution room-temperature spectrum also shows partially defined splitting from the axial nitrogens, in a rough 1:2:3:2:1 intensity ratio, as observed in the $g_{\parallel}$ region of the frozen-solution spectrum. Hence, the coordinated groups are the same in both phases. We have observed that many different types of nickel(III) complexes[8,20,22] have g_{iso} values in aqueous solutions that are consistently larger (by 0.009 ± 0.004) than g_{av} values for the frozen glassy state. This appears to be due to the change in phase rather than the change in temperature. The same ligands are coordinated in both phases, but the surrounding environment is slightly different.

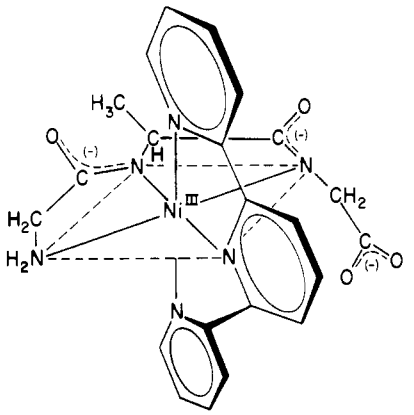

2

A characteristic of the EPR spectra for these mixed-ligand complexes is the shift in g values associated with the number and strength of axial donor groups. Increased donor strength and bond compression along the z axis result in a corresponding elongation and weakening of the bonds along the x and y axes.[22] This is observed in a shift from $g_{\perp} = 2.264$ for the two axial waters of $Ni^{III}(H_{-2}GAG)(H_2O)_2$, to $g_{\perp} = 2.190$ and finally to $g_{\perp} = 2.168$ for the bpy and terpy mixed-ligand complexes, respectively. This decrease in the $g_{\perp}$ values is observed in the mono- and bis(ammine)nickel(III) peptide complexes[6] and in the case of the five- and six-nitrogen bis(tripeptide)nickel(III) complexes.[8]

Shifts in the $g_{\parallel}$ values are observed, and stronger axial donors lead to slightly higher values. This is due to vibronic mixing of the d_{z^2} and $d_{x^2-y^2}$ ground states as the complex approaches an octahedral geometry.[3] Typical $g_{\parallel}$ values for complexes with two axial waters, a water and an amine nitrogen, and two amine nitrogens are 2.010, 2.015, and 2.020, respectively. The polypyridine complexes follow this trend (Table II).

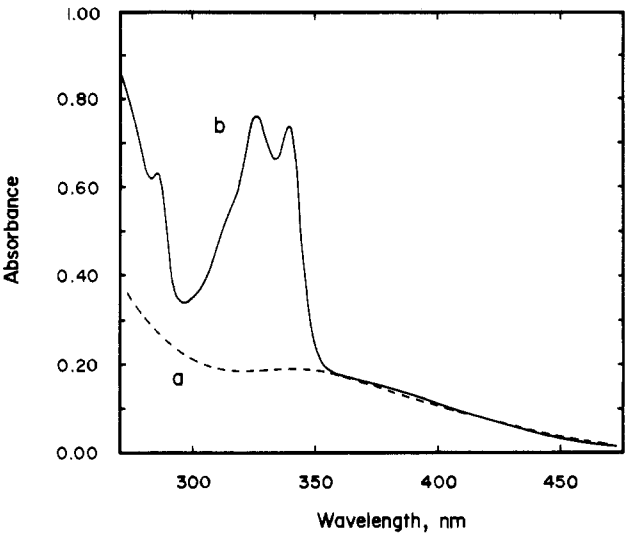

Figure 4. UV–visible spectra (1-cm cell, pH 5, 0.1 M $NaNO_3$, 4.5×10^{-5} M Ni(III)): (a) $Ni^{III}(H_{-2}GAG)(H_2O)_2$; (b) $Ni^{III}(H_{-2}GAG)$terpy.

The symmetry of the EPR line shape is also important in the assignment of structures to these complexes. The $Ni^{III}(H_{-2}GAG)(H_2O)_2$ complex has different values for g_{xx} and g_{yy} (Table II), which reflect the different donors along the equatorial axes (structure **1**). In this case, the peptide donors along the y axis are an amine NH_2 and a deprotonated peptide nitrogen N(−), while along the x axis the donors are a N(−) and a terminal carboxylate group. As the interaction of chelated axial nitrogen donors on the line shape of the equatorial region is taken into account, the spectra can be simulated with g_{xx} and g_{yy} values that are equivalent. This, in turn, assumes that the two pairs of donor groups along the axes defined as x and y in structure **1** are equivalent (e.g. the terminal amine and the deprotonated peptide nitrogen N(−) along the y axis are equivalent to the N(−) and pyridine nitrogen along the x axis). This is borne out in the peak symmetry of the $g_{\perp}$ region for both the bpy and terpy complexes, as opposed to the shoulder observed for the parent tripeptide complex. For complexes with symmetrical $g_{\perp}$ regions, g_{xx} and g_{yy} are assumed to be equal and are reported as $g_{\perp} = {}^1/_2(g_{xx} + g_{yy})$. Better fits of the computer simulation to the data are not accomplished with different g_{xx} and g_{yy} values.

In general, the hyperfine coupling constants also decrease with an increase in the number of N donors. Four and five N donors tend to have A_{zz} values of ~24 G, while six N donors have A_{zz} values of ~20 G.

UV–Vis Spectrum of $Ni^{III}(H_{-2}GAG)$terpy. It is difficult to observe directly the UV–vis spectrum of the $Ni^{III}(H_{-2}GAG)$terpy complex because of interference from the $Ni^{II}(terpy)_2^{2+}$ complex. Nickel(II) forms very stable mono- and bis(terpyridine) complexes, with values of log $K_1 = 10.7$ and log $K_2 = 11.1$, respectively.[23] The efficiency of the bulk electrolysis column used to oxidize the nickel(II) complexes is 50–70% for most nickel(II) glycyl and L-alanyl tripeptide complexes. At pH 5 any remaining $Ni^{II}(H_{-2}GAG)^-$, as well as any nickel(II) species formed from the redox decomposition of $Ni^{III}(H_{-2}GAG)(H_2O)_2$, rapidly dissociates to give free peptide and aqueous nickel(II). Under the above conditions, with $[Ni^{III}(H_{-2}GAG)(H_2O)_2] \sim [Ni^{2+}(aq)]$, the $Ni^{III}(H_{-2}GAG)$terpy solution will also contain some $Ni(terpy)_2^{2+}$. This bis(terpyridine) complex has strong absorption bands at 334 nm ($\epsilon = 3.2 \times 10^4$ M^{-1} cm^{-1}) and 320 nm ($\epsilon = 3.6 \times 10^4$ M^{-1} cm^{-1}).[23] The UV–vis spectrum of $Ni^{III}(H_{-2}GAG)$terpy is shown in Figure 4. A cation-exchange column is used to remove all $Ni(terpy)_2^{2+}$ in order to eliminate this interference. The nickel(III) peaks are at 326 nm ($\epsilon \sim 1.6 \times 10^5$ M^{-1} cm^{-1}) and 339 nm ($\epsilon \sim 1.5 \times 10^5$ M^{-1} cm^{-1}).

(23) Holyer, R. H.; Hubbard, C. D.; Kettle, S. F. A.; Wilkins, R. G. *Inorg. Chem.* **1966**, *5*, 622–625.

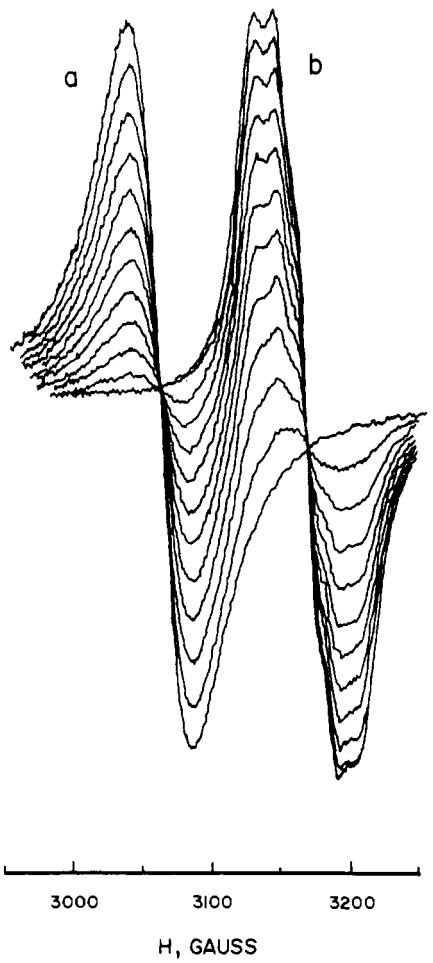

Figure 5. Aqueous-solution room-temperature EPR spectra: (a) $Ni^{III}(H_{-2}GAG)(H_2O)_2$; (b) $Ni^{III}(H_{-2}GAG)$terpy. The decrease in the $Ni^{III}(H_{-2}GAG)(H_2O)_2$ signal and increase in the $Ni^{III}(H_{-2}GAG)$terpy signal are functions of the increasing terpy concentration.

Aqueous EPR Titration To Determine the Terpy Stability Constant. Full formation of the $Ni^{III}(H_{-2}GAG)$terpy complex is observed by EPR when the terpy concentration is equal to the total nickel concentration, which implies that the terpy complex has a large stability constant. A potentiometric titration is not possible because of nickel(III) decomposition, nor could the stability constant be determined by spectrophotometric titration due to the interference of $Ni(terpy)_2^{2+}$. The stability constant for $Ni^{III}(H_{-2}GAG)$terpy

$$K = \frac{[Ni^{III}(H_{-2}GAG)terpy]}{[Ni^{III}(H_{-2}GAG)(H_2O)_2][terpy]} \quad (1)$$

was determined by aqueous titration with the EPR as a detector. The aqueous-solution EPR signals of $Ni^{III}(H_{-2}GAG)(H_2O)_2$ and $Ni^{III}(H_{-2}GAG)$terpy are easily distinguished (Figure 5) and provide a means to determine the concentration of the nickel(III) species, without interference from the diamagnetic nickel(II) species.

The free terpy concentration is more difficult to determine, as it can coordinate to either the nickel(III) peptide or nickel(II). In addition, as $Ni^{III}(H_{-2}GAG)(H_2O)_2$ has a half-life of only 45 min at this pH, an appreciable amount of nickel(III) decomposes over the time required to carry out the titration. This leads to an ever changing nickel(II) concentration. To overcome this problem, titration experiments were performed with a large excess of nickel(II) (0.020 M Ni^{2+}(aq) with 4.0×10^{-4} M $Ni^{III}(H_{-2}GAG)(H_2O)_2$) so that the aquonickel(II) concentration was essentially constant except for dilution. The free terpy concentration was determined from the concentration of terpy added, the pH, the total nickel(II) and nickel(III) concentrations, and the nickel(II) terpy stability constants.

The initial nickel(III) peptide concentration, $[Ni^{III}(H_{-2}GAG)(H_2O)_2]_0$, was determined by the visible absorbance ($\epsilon_{341} = 4230\ M^{-1}\ cm^{-1}$)[24] of an aliquot of the solution to be titrated. The absorbance of this aliquot was monitored continuously during the experiment. Thus the $Ni^{III}(H_{-2}GAG)(H_2O)_2$ concentration could be calculated at any time. The concentration of $Ni^{III}(H_{-2}GAG)(H_2O)_2$, determined from the height of the EPR derivative signal, $[Ni^{III}(H_{-2}GAG)(H_2O)_2]_{EPR}$, is equal to the EPR response at time t, R_t, divided by the response at the time of the first absorbance measurement, R_0, times $[Ni^{III}(H_{-2}GAG)(H_2O)_2]_0$:

$$[Ni^{III}(H_{-2}GAG)(H_2O)_2]_{EPR} = \frac{R_t}{R_0}[Ni^{III}(H_{-2}GAG)(H_2O)_2]_0 \quad (2)$$

The concentration of the terpy complex, $[Ni^{III}(H_{-2}GAG)terpy]_t$, is the difference between the nickel(III) concentration expected with only decomposition taken into account and the nickel(III) concentration measured from the EPR data:

$$[Ni^{III}(H_{-2}GAG)terpy]_t = [Ni^{III}(H_{-2}GAG)(H_2O)_2] - [Ni^{III}(H_{-2}GAG)(H_2O)_2]_{EPR} \quad (3)$$

The decay of the $Ni^{III}(H_{-2}GAG)$terpy complex is small over the time of the experiment (~15 min). The concentration of terpy not bound to nickel(III), $[terpy]_t$, is

$$[terpy]_t = [terpy]_0 - [Ni^{III}(H_{-2}GAG)terpy]_t \quad (4)$$

where $[terpy]_0$ is the concentration of terpy added, with no complexation.

The free terpy concentration was then determined from the COMICS program,[25] with the following complex formation[23] and protonation[26] equilibria taken into account:

$$Hterpy^+ \rightleftarrows terpy + H^+ \qquad pK_a = 4.64 \quad (5)$$

$$H_2terpy^{2+} \rightleftarrows Hterpy^+ + H^+ \qquad pK_a = 3.42 \quad (6)$$

$$Ni^{2+} + terpy \rightleftarrows Ni(terpy)^{2+} \qquad \log K_1 = 10.7 \quad (7)$$

$$Ni(terpy)^{2+} + terpy \rightleftarrows Ni(terpy)_2^{2+} \qquad \log K_2 = 11.1 \quad (8)$$

Data were collected for several terpy concentrations, and an average value of $\log K = 12.8 \pm 0.4$ (pH 5.0, $\mu = 0.1$ ($NaNO_3$)) was calculated for the $Ni^{III}(H_{-2}GAG)$terpy complex (eq 1). This stability constant is 10^{11} times greater than that for the mono(pyridine)nickel(III) peptide complexes reported earlier,[4] and this reflects the additional stability from the formation of chelate rings.

The $Ni^{III}(H_{-2}GAG)(H_2O)$bpy complex forms rapidly in aqueous solution. Addition of 10^{-2} M Ni^{2+}(aq) at pH 5 results in displacement of the bpy to form $Ni(bpy)^{2+}$ and $Ni^{III}(H_{-2}GAG)(H_2O)_2$. Terpy also rapidly displaces bpy to form $Ni^{III}(H_{-2}GAG)$terpy, which indicates that the bidentate bpy does not form as stable a complex as does the tridentate ligand. The Ni^{2+}(aq) ion at 10^{-2} M (pH 5) does not displace terpy from $Ni^{III}(H_{-2}GAG)$terpy at a rate that is distinguishable from the rate of redox decomposition of this species.

Kinetic Stability. Formation of nickel(III) tripeptide axial donor species leads to complexes that are more stable than the parent nickel(III) complex with regard to redox decomposition in neutral and basic solutions. Table III gives first-order rate constants for the decomposition of the $Ni^{III}(H_{-2}GAG)$terpy complex. The reactions gave pseudo-first-order behavior over 4 half-lives. The chelated terpy greatly stabilizes the nickel(III) tripeptide species compared to the diaqua complex, as evidenced by the 10^6-fold decrease in the rate of redox decomposition at pH 11.

Plots of the log of the rate constants for the acid decomposition of $Ni^{III}(H_{-2}GAG)(H_2O)_2$ and for the base decomposition of $Ni^{III}(H_{-2}GGA)(H_2O)_2$ are compared with a plot for the $Ni^{III}(H_{-2}GAG)$terpy complex in Figure 6. The behavior of the GAG

(24) Murray, C. K.; Margerum, D. W., unpublished results.
(25) Perrin, D. D.; Sayce, I. G. *Talanta* **1967**, *14*, 833–842.
(26) Smith, R. M.; Martell, A. E. "Critical Stability Constants"; Plenum Press: New York, 1982; Vol. 5.

Table III. Rate Constants for the Decomposition of $Ni^{III}(H_{-2}GAG)$terpy as a Function of −log $[H^+]$[a]

−log $[H^+]$	buffer	$10^5 k_{obsd}$, s^{-1}	−log $[H^+]$	buffer	$10^5 k_{obsd}$, s^{-1}
11.8	phosphate	13.5 ± 0.1	3.62	phosphate	2.57 ± 0.01
9.61	borate	8.51 ± 0.03	3.21	phosphate	1.87 ± 0.01
7.30	phosphate	3.34 ± 0.05	2.00	$HClO_4$	6.75 ± 0.01
5.33	acetate	1.29 ± 0.01	1.31	$HClO_4$	2.55 ± 0.01
4.86	acetate	4.40 ± 0.01	1.00	$HClO_4$	4.13 ± 0.01

[a] Buffer concentrations 0.01 M, λ 360 nm, μ 0.1 ($NaClO_4$ or $NaNO_3$), 25.0 °C.

or GGA complexes of Ni(III) in base are similar. Above pH 11 the $Ni^{III}(H_{-2}GGA)(H_2O)_2$ reactions showed good first-order kinetics. However, below pH 11 the kinetics data became complicated as the reaction proceeded. At pH 9–11 axial coordination of excess peptide or peptide fragments (due to self-redox decomposition) is likely a source of interference.[5,8] These ligands tend to stabilize the nickel(III) complex and lead to more complicated kinetics. Therefore first-order rate constants were calculated from the initial reaction rates, taken over the first 25% of the reaction. In the acidic region the rate of decomposition of the mixed-ligand species is roughly that of the parent complex. Its reactions are approximately first-order in nickel(III) and first order in $[H^+]$.[27]

Electrode Potential of $Ni^{III,II}(H_{-2}GAG)$terpy$^{0,-}$. Cyclic voltammograms of most of the nickel(III) polypyridine mixed-ligand complexes show only a reductive wave and no reverse oxidation wave. This is true for the $Ni^{III}(H_{-2}GAG)$terpy complex at pH 5–10; however, an oxidative wave is observed at pH 12–13. The CV peak to peak separation is 76 mV at pH 13 and the $E°'$ value of 0.56 ± 0.01 V (vs. NHE) is independent of scan rate (20–400 mV s^{-1}). The peak currents are proportional to the square root of the scan rate, which indicates that the complex is not adsorbed onto the electrode. The same $E°'$ value was obtained at pH 12 and 13 by Osteryoung square-wave voltammetry.[28]

The following thermodynamic cycle gives the value of $10^{8.1}$ M^{-1} for the nickel(II) ternary stability constant, K':

$$Ni^{III}(H_{-2}GAG) + terpy \underset{}{\overset{K=10^{12.8}}{\rightleftharpoons}} Ni^{III}(H_{-2}GAG)terpy \quad (9)$$

$$\Big\Vert +e^-, E°' = 0.84\ V \qquad \Big\Vert +e^-, E°' = 0.56\ V$$

$$Ni^{II}(H_{-2}GAG)^- + terpy \underset{}{\overset{K'}{\rightleftharpoons}} Ni^{II}(H_{-2}GAG)terpy^- \quad (10)$$

The concentrations of metal ion complex species (COMICS)[25] were calculated for the known nickel(II) species of G_3^- and terpy as a function of pH. The constants for the mono- and bis(terpyridine) complexes are given in eq 7, 8, and 10. The G_3 stability constants with nickel(II)[29] are β_{011} 7.89, β_{101} 3.71, β_{1-11} −5.09, β_{1-21} −12.82, β_{1-31} −25.62, and β_{102} 6.81. The COMICS calculations (with the assumption that the GAG and G_3 stability constants are similar) show that $Ni^{II}(H_{-2}GAG)terpy^-$ will not be present in appreciable concentrations below pH 10. This ternary complex does become a predominant species in solution above pH 12.

At pH 5–8 $Ni^{II}(H_{-2}GAG)terpy^-$ formed by electrochemical reduction rapidly loses GAG. Hence no oxidative wave is seen for this complex even at scan rates as high as 2 V s^{-1}. The reductive wave of the nickel(III) complex also becomes poorly defined and shifts to lower potentials at these high scan rates due to slow heterogeneous electron transfer. At pH 8–10 a $E°'$ value of 0.54 ± 0.01 V (scan rates 20–400 mV s^{-1}) can be estimated from the reductive wave and an oxidative inflection that is present due to small amounts of $Ni^{II}(H_{-2}GAG)terpy^-$. At pH 8–10 the COMICS distribution indicates that this ternary complex dissociates into a mixture of $Ni^{II}(H_{-2}GAG)^-$, GAG^-, and $Ni(terpy)_2^{2+}$.

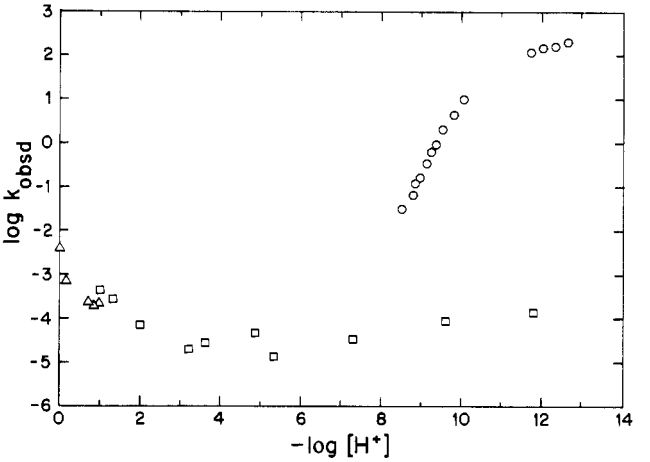

Figure 6. Dependence of the decomposition rate constant (k_{obsd}, s^{-1}) on −log $[H^+]$ at 25 °C: (□) $Ni^{III}(H_{-2}GAG)$terpy, μ = 0.1 ($NaNO_3$); (○) $Ni^{III}(H_{-2}GGA)(H_2O)_2$, μ = 1.0 ($NaClO_4$); (△) $Ni^{III}(H_{-2}GAG)(H_2O)_2$, μ = 1.0 ($NaClO_4$).

Another pair of CV waves appears with repeated scans at high pH and gives an $E°'$ value of 0.67 V. This is an adsorbed species that can be removed by reconditioning the electrode. A similar species was found in studies[8] of $Ni^{III}(H_{-2}G_3)_2^{3-}$, where no terpy was present.

The potential for the ternary complex is 0.28 V lower than the $Ni^{III,II}(H_{-2}GAG)(H_2O)_2^{0,-}$ potential[17] and is at least 1.1 V lower than the potential for the $Ni^{III,II}(terpy)_2^{3+,2+}$ couple that is estimated from the $Ni^{III,II}(bpy)_3^{3+,2+}$ potential to be about 1.7 V in aqueous solution.[14] The mixed-ligand complex with both $H_{-2}GAG$ and terpy coordinated to nickel(III) has a relatively low reduction potential for Ni(III,II) couples and is a stable complex both thermodynamically and kinetically.

Acknowledgment. This work was supported by Public Health Service Grant No. GM-12152 from the National Institutes of General Medical Sciences.

Registry No. $Ni^{III}(H_{-2}GGA)(H_2O)_2$, 99213-00-0; $Ni^{III}(H_{-2}GGA)(H_2O)$en (monodentate), 99213-01-1; $Ni^{III}(H_{-2}GGA)(en)_2$ (monodentate, bidentate), 99213-02-2; $Ni^{III}(H_{-2}GGA)(H_2O)$dien (monodentate), 99213-03-3; $Ni^{III}(H_{-2}GGA)(H_2O)$dien (bidentate), 99213-04-4; $Ni^{III}(H_{-2}GGA)$dien (tridentate), 99213-05-5; $Ni^{III}(H_{-2}Aib_3)(H_2O)_2$, 76757-47-6; $Ni^{III}(H_{-2}Aib_3)(H_2O)$en (monodentate), 99213-06-6; $Ni^{III}(H_{-2}Aib_3)(H_2O)$dien (monodentate), 99232-37-8; $Ni^{III}(H_{-2}Aib_3)(H_2O)NH_3$, 99213-12-4; $Ni^{III}(H_{-2}Aib_3)(NH_3)_2$, 99213-13-5; $Ni^{III}(H_{-2}GAG)(H_2O)_2$, 99213-07-7; $Ni^{III}(H_{-2}GAG)(H_2O)$bpy (bidentate), 99213-08-8; $Ni^{III}(H_{-2}GAG)(H_2O)$phen (bidentate), 99213-09-9; $Ni^{III}(H_{-2}GAG)(H_2O)Ph_2$phen (bidentate), 99213-10-2; $Ni^{III}(H_{-2}GAG)$(terpy) (tridentate), 99213-11-3; $Ni^{II}(H_{-2}GAG)$(terpy) (tridentate), 99213-14-6.

(27) Loyola, V. H.; Subak, E. J.; Margerum, D. W., to be submitted for publication.
(28) Kissinger, P. T.; Heineman, W. R. "Laboratory Techniques in Electroanalytical Chemistry"; Marcel Dekker: New York, 1984.
(29) Billo, E. J.; Margerum, D. W. *J. Am. Chem. Soc.* **1970**, *92*, 6811–6818.